J Sol-Gel Sci Technol (2011) 58:501–506
DOI 10.1007/s10971-011-2419-6

ORIGINAL PAPER

The microstructure and magnetic properties of $Ni_{0.4}Zn_{0.6}Fe_2O_4$ films prepared by spin-coating method

Tao Yuan · Zhonglei Wei · Jing Yuan · Longgang Yan · Qingfang Liu · Jianbo Wang

Received: 4 November 2010 / Accepted: 2 February 2011 / Published online: 15 February 2011

Abstract Nickel zinc ferrite ($Ni_{0.4}Zn_{0.6}Fe_2O_4$) films on Si (100) substrate were synthesized using a spin-coating method. The crystallinity of the $Ni_{0.4}Zn_{0.6}Fe_2O_4$ films with the thickness of about 386 nm became better as the annealing temperature increased. The films have smooth surface, relatively good packing density and uniform thickness. The volatilization of Zn is serious at 900 °C. With the increase of annealing temperature, the saturation magnetization M_s increases in the temperature ranging from 400 to 700 °C, however, decreases above 700 °C, and the coercivity H_c increases in the temperature range 400–800 °C, decreases above 800 °C. After annealed at 700 °C for 2 h in air with the heating rate 2 °C/min, the film shows a maximum saturation magnetization M_s of 349 emu/cc and low coercivity H_c of 66 Oe. The M_s is higher than others which prepared by this method, however, the H_c is lower. The M_s of $Ni_{0.4}Zn_{0.6}Fe_2O_4$ films annealed at 700 °C increases with increasing annealing time and the H_c changes slightly.

Keywords $Ni_{0.4}Zn_{0.6}Fe_2O_4$ films · Spin-coating method · Magnetic property · Volatilization of Zn

1 Introduction

Spinel type Ni–Zn ferrites are of great interest due to their potential applications in microelectronics, magneto-optics and microwave device. Many methods, such as sputtering [1–3], pulsed laser deposition (PLD) [4], spin-spray [5–7], chemical co-precipitation method [8–10], combustion method [11–13], hydrothermal method [14, 15] and sol–gel method [16–18] which are used to fabricate Ni–Zn ferrites films. Among them, sol–gel spin-coating method has unique advantages such as excellent composition control and low temperature process. Moreover, microstructure and grain size of thin films can be controlled by annealing temperature. Besides, the equipment is cheap and the high vacuum is not necessary.

Bulk Ni–Zn ferrite has been intensely studied due to its remarkable magnetic properties and low production cost. However, the Ni–Zn ferrite employed in discrete devices at microwave frequency is not compatible with the rapid developments of electronic applications with miniaturation, high density, integration and multifunction. To solve these difficulties in performing the required miniaturization for complex devices, special focus has been placed on Ni–Zn ferrite films. The ferrite films play an important role in facilitating the design and fabrication of devices such as micro-inductors, micro-transformers and electromagnetic interference (EMI) suppressors, due to their chemical stability and mechanical resistance, as well as their low eddy current loss and high resistivity. In addition, they are essential in read-head technology, and in the fabrication of micro-transformers or electromagnetic noise suppressors. Deposited on semiconductors, they are also considered as good non-reciprocal components on a microwave monolithic integrated circuit. The ferrite films incorporated into magnetic integrated circuits are expected to replace the current surface mounting modules in the near future.

In this paper, $Ni_{0.4}Zn_{0.6}Fe_2O_4$ films were fabricated using spin-coating method. The composition $Ni_{0.4}Zn_{0.6}Fe_2O_4$ was selected because its magnetic properties are superior to those of other composition in $Ni_xZn_{1-x}Fe_2O_4$

T. Yuan · Z. Wei · J. Yuan · L. Yan · Q. Liu (✉) · J. Wang
Key Laboratory for Magnetism and Magnetic Materials of Ministry of Education, Lanzhou University, Lanzhou 730000, People's Republic of China
e-mail: liuqf@lzu.edu.cn

($0 \leq x \leq 1$) system in previous report [3, 19]. The effects of the structural properties, composition, crystallization temperature and annealing time on magnetic properties of the Ni–Zn thin films were investigated.

2 Experimental

The $Ni_{0.4}Zn_{0.6}Fe_2O_4$ films were prepared by spin-coating method. Analytical grade nickel acetate ($Ni(CH_3COO)_2 \cdot 4H_2O$) (3.2 mmol), zinc acetate ($Zn(CH_3COO)_2 \cdot 2H_2O$) (4.8 mmol) and iron nitrate ($Fe(NO_3)_3 \cdot 9H_2O$) (16.0 mmol) were used as starting chemicals. The above three chemicals were dissolved in 2-methoxyethanol to form a mixed solution. The concentration of the solution was adjusted to 0.2 mol/L by 2-methoxyethanol. The solution was stirred for 3 h and placed for 24 h at room temperature to form the stable precursor used for following process. Then the wet films were deposited by spin-coating method with 5,000 rpm for 40 s on Si (100) substrates. The obtained films were dried at 120 °C for 5 min to remove the mixed solvents, and then heated at 400 °C for 5 min to pyrolyze and exclude the organic substances. The operation of spin-coating, drying and heating were repeated to get the required thickness of the films. Finally, the as-deposited films were annealed at 400 °C for 120 min in the air and cooled slowly in the furnace. The thickness of the films was about 386 nm with 10 layers. And the $Ni_{0.4}Zn_{0.6}Fe_2O_4$ films annealed at the temperatures ranging from 400 to 900 °C for 120 min.

The phase identification of the films was performed by X-ray diffraction (XRD) on a Rigaku D/Max-2400 with Cu K_α radiation. The surface morphologies and thickness of the films were characterized by scanning electron microscopy (SEM) on a Hitachi S-4800, which is equipped with an energy-dispersive X-ray spectrometer (EDS). Static magnetic measurement was carried out on a Lakeshore vibrating sample magnetometer (VSM) with a maximum magnetic field of 12 kOe. The direction of the applied magnetic field was parallel to the film plane.

3 Results and discussion

The XRD patterns of $Ni_{0.4}Zn_{0.6}Fe_2O_4$ films were annealed at different temperatures (400, 500, 600, 700, 800 and 900 °C) for 120 min are shown in Fig. 1. There are characteristic peaks of spinel Ni–Zn ferrites in X-ray patterns of all samples, which exhibits the Ni–Zn ferrites are the main crystalline phases. The well-defined peaks corresponding to cubic spinel ferrite also increase and the crystallinity of the ferrite films become better with increasing annealing temperature.

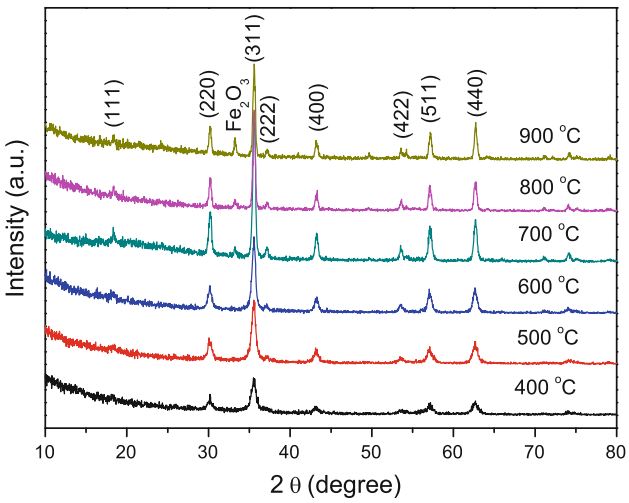

Fig. 1 XRD patterns of $Ni_{0.4}Zn_{0.6}Fe_2O_4$ films annealed at 400, 500, 600, 700, 800 and 900 °C for 120 min

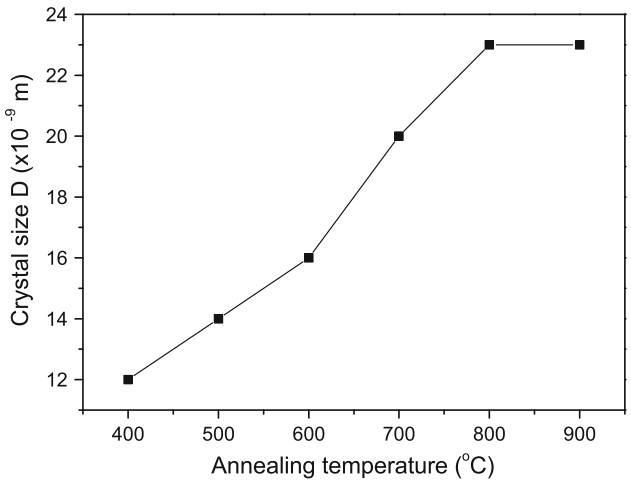

Fig. 2 Crystal size D of $Ni_{0.4}Zn_{0.6}Fe_2O_4$ as a function of annealing temperature T

Figure 2 shows the crystal size for $Ni_{0.4}Zn_{0.6}Fe_2O_4$ films annealed at various temperatures. The average crystal size was calculated by the Scherrer equation from the broadening (311) peaks of spinel [20],

$$D = \frac{0.9\lambda}{\beta \cos\theta} \quad (1)$$

where D, λ, β, θ are the crystal size, X-ray wavelength, the full width at half maximum value and the diffraction angle, respectively. The average crystal size of all samples increases with annealing temperature. When the annealing temperature increases, $Ni_{0.4}Zn_{0.6}Fe_2O_4$ grains with higher energy have enough mobility on the thermal substrate.

Figure 3 shows the SEM images of the surface topography and cross section of the $Ni_{0.4}Zn_{0.6}Fe_2O_4$ films annealed at different temperatures. It is clearly seen that the

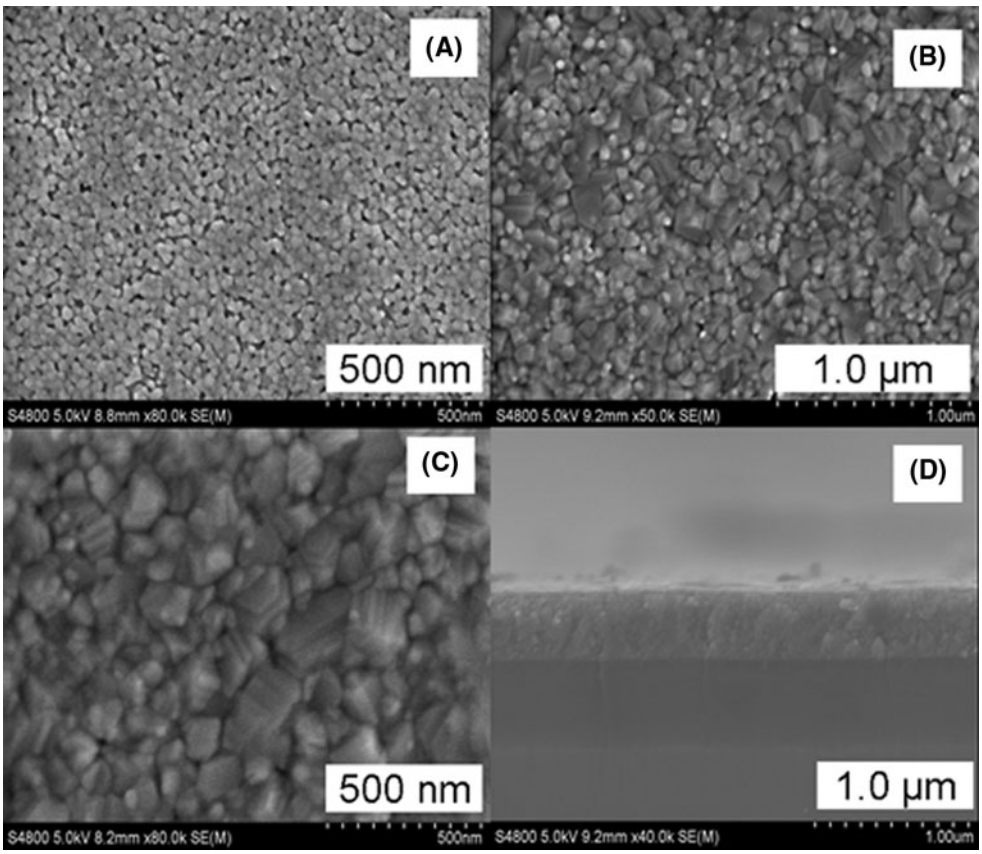

Fig. 3 SEM images of $Ni_{0.4}Zn_{0.6}Fe_2O_4$ films annealed at different temperatures: **a** 600 °C, **b** 800 °C, **c** 900 °C, **d** is the cross-sectional SEM micrographs of films annealed at 600 °C

grain size increases with increasing the annealing temperature. As seen from Fig. 3a, the film annealed at 600 °C shows a dense film structure, a smooth surface and a relatively good packing density. It is observed that some porosities emerge on the surface of the film after annealing. The mean grain size is about 30 nm, 70 nm and 100 nm for the films annealed at 600, 800 and 900 °C, respectively, the grain size is strongly dependent on the annealing temperature. Moreover, the grain size is rather uniform and the film appears to be dense with a rather smooth surface. SEM images of the films show no any crack. Estimated from Fig. 3d, the thickness annealed at 600 °C is 386 nm and the film has good adhesion to substrates.

Figure 4 shows Energy dispersive absorption spectroscopy of $Ni_{0.4}Zn_{0.6}Fe_2O_4$ films annealed at different temperatures. The peaks of the elements Ni, Zn, Fe, and O were observed and have been assigned. The Atom Conc % of Ni and Zn of the films annealed at different temperatures are given in Table 1. The Atom Conc % content of Ni and Fe keep steady. However, the Atom Conc % content of Zn decreases from 6.05 at 600 °C to 3.88 at 900 °C. This phenomenon consists with Sharma et al. [21], which shows the volatilization of Zn is very serious at high temperatures.

Figure 5 shows the magnetic hysteresis loops of the samples annealed at different temperatures, using a vibrating-sample magnetometer (VSM) measured at room temperature with 12 kOe to reach saturation values. With the increase of annealing temperature, the saturation magnetization M_s increase in the temperature ranging from 400 to 700 °C, decrease above 700 °C, and the coercivity H_c increase in the temperature ranging from 400 to 800 °C, decrease above 800 °C. After annealed at 700 °C for 2 h in air with the heating rate 2 °C/min, the film shows a maximum saturation magnetization M_s 349 emu/cc and low coercivity H_c 66 Oe. The M_s is higher than others which prepared by this method, however, the H_c is lower.

The results can be explained by grain growth and volatilization of zinc in $Ni_{0.4}Zn_{0.6}Fe_2O_4$ films. The increase of annealing temperature results in an enhancement of crystallization, an increase of grain size, and a decrease of volume of grain boundary, which help promote the magnetization of $Ni_{0.4}Zn_{0.6}Fe_2O_4$ films and thus lead to an increase of M_s. However, above 700 °C, the decrease of M_s is probably due to volatilization of zinc as is demonstrated in EDS. Figure 6b presents the annealing temperature dependence of the coercivity H_c. It is found that the H_c

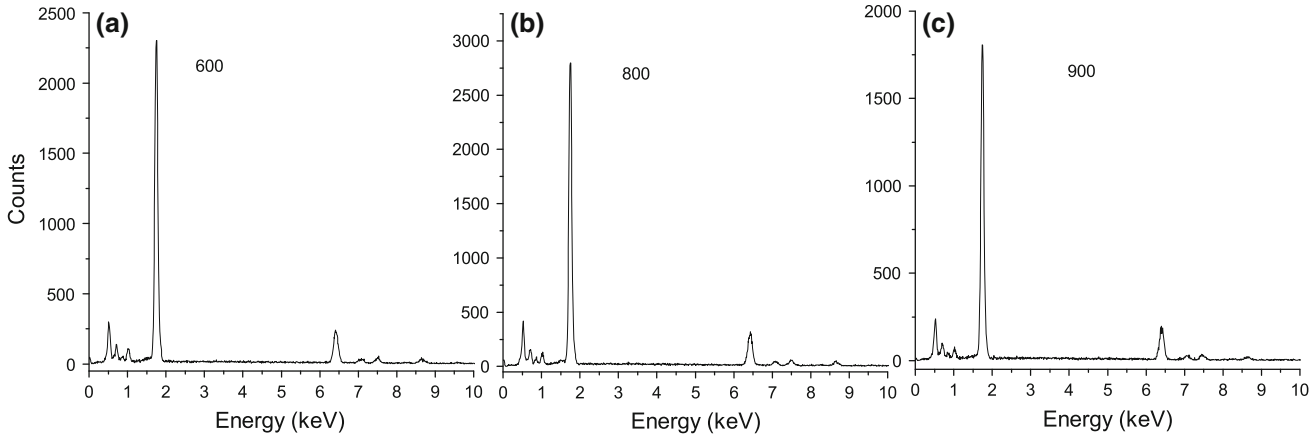

Fig. 4 Energy dispersive absorption spectroscopy photograph of $Ni_{0.4}Zn_{0.6}Fe_2O_4$ films annealed at different temperatures: **a** 600 °C, **b** 800 °C, and **c** 900 °C

Table 1 The atom conc % of Ni and Zn of the films annealed at different temperatures: (A) 600 °C, (B) 800 °C, and (C) 900 °C

Temperature (°C)	Atom conc % of Ni	Atom conc % of Zn	Atom conc % of Fe
600	4.45	6.05	19.13
800	4.38	5.22	19.55
900	4.88	3.88	19.45

enhanced with the increasing annealing temperature and then decreases when the temperature is 900 °C. To understand H_c mechanism clearly, the critical single domain size can be estimated by the following formula [22],

$$D_m = \frac{9\sigma_w}{2\pi M_s^2} \tag{2}$$

where $\sigma_w = (2k_B T_c |k_1|/a)^{1/2}$, k_1, T_c, M_s, k_B, a are the wall density energy, magnetocrystalline anisotropy constant, Curie temperature, Boltzmann constant and lattice constant, respectively. For $Ni_{0.4}Zn_{0.6}Fe_2O_4$ film, $M_s = 270$ Gs, $T_c = 860$ K, $a = 8.4 \times 10^{-8}$ cm, and $|k1| = 6.5 \times 10^4$ erg/cm^3 [23], which give the value of D_m about 70 nm. The calculated value is larger than that of samples below 800 °C, but smaller than the sample annealed at 900 °C.

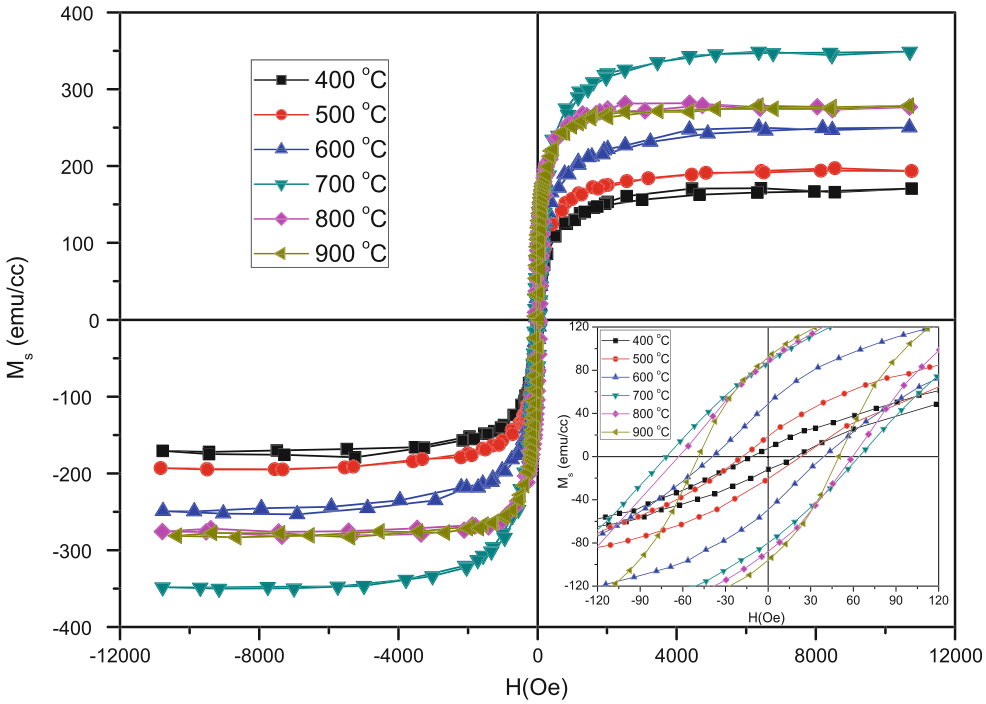

Fig. 5 The magnetic hysteresis loops of the $Ni_{0.4}Zn_{0.6}Fe_2O_4$ films annealed at 400, 500, 600, 700, 800 and 900 °C for 120 min, recorded at room temperature. *Inset*: the expanded of the magnetic hysteresis loops

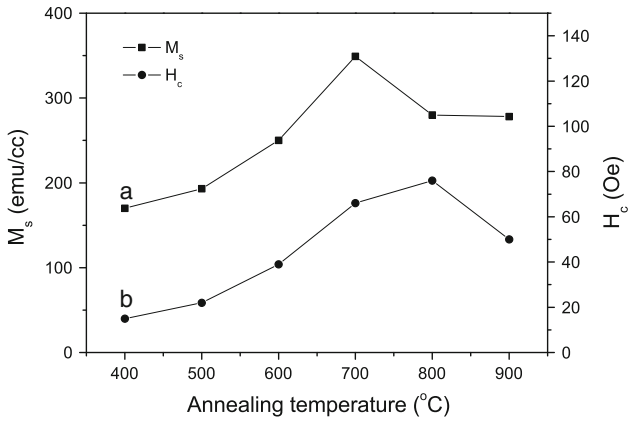

Fig. 6 The dependence of the M_s on annealing temperature of the $Ni_{0.4}Zn_{0.6}Fe_2O_4$ films (*a*) and the H_c as functions of annealing temperature (*b*)

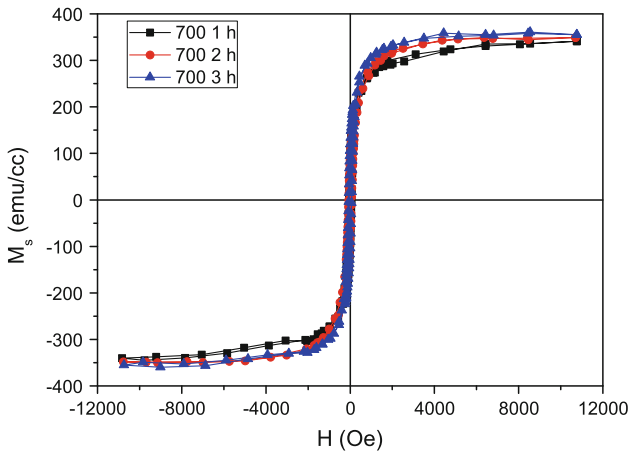

Fig. 7 The magnetic hysteresis loops of the $Ni_{0.4}Zn_{0.6}Fe_2O_4$ films annealed at 700 °C, for different annealing time (1, 2 and 3 h), recorded at room temperature

Therefore, the H_c initially increases and then decreases as the annealing temperature increases.

Figure 7 shows the M_s and H_c of $Ni_{0.4}Zn_{0.6}Fe_2O_4$ films annealed at 700 °C for different annealing time. The M_s and the H_c increase with increasing annealing time. In combination with the previous analyses about crystal structure and surface morphology, it is not difficult to understand the change of M_s and H_c. It can be explained by grain growth of $Ni_{0.4}Zn_{0.6}Fe_2O_4$ films. Figure 8 presents the M_s is better with the increase of calcination time, however, the H_c changes slightly. The increase of annealing time results in an enhancement of crystallization, and a decrease of volume of grain boundary, which help promote the magnetization of the films and thus lead to an increase of M_s.

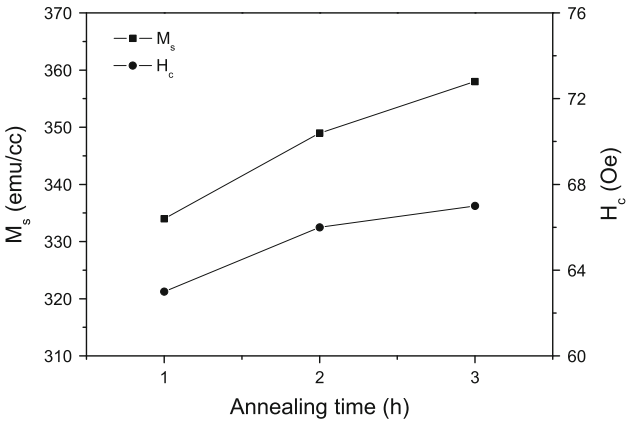

Fig. 8 The dependence of the M_s and H_c of $Ni_{0.4}Zn_{0.6}Fe_2O_4$ films annealed at 700 °C for different annealing time (1, 2 and 3 h)

4 Conclusions

Nickel zinc ferrite $Ni_{0.4}Zn_{0.6}Fe_2O_4$ films have been synthesized using a spin-coating sol–gel process. The film has a smooth surface, a relatively good packing density and uniform thickness, and the volatilization of zinc is very serious at high temperature. With the increase of annealing temperature, the saturation magnetization M_s increases in the temperature ranging from 400 to 700 °C, decreases above 700 °C, and the coercivity H_c increases in the temperature ranging from 400 to 800 °C, decreases above 800 °C. After annealed at 700 °C for 2 h in air with the heating rate 2 °C/min, the film shows a maximum saturation magnetization M_s of 349 emu/cc and low coercivity H_c of 66 Oe. The M_s is higher than others which prepared by this method, however, the H_c is lower. The M_s is better with the increase of calcination time at 700 °C, however, the H_c changes slightly.

Acknowledgments This work is supported by the National Natural Science Foundation of China (11074101), program for New Century Excellent Talents (NCET) in University and the Fundamental Research Funds for the Central Universities (860080).

References

1. Guo D, Fan X, Chai G, Jiang C, Li X, Xue D (2010) Appl surf Sci 256:2319
2. Prado J, Gómez ME, Prieto P, Mendoza A (2009) J Mag Mag Mater 321:2792
3. Dangwei G (2009) J Phys D Appl Phys 42:125006
4. Ravinder D, Vijay Kumar K, Ramana Reddy AV (2003) Mater Lett 57:4162
5. Beji Z, Smiri LS, Vaulay MJ, Herbst F, Ammar S, Fiévet F (2010) Thin Solid Films 518:2592
6. Beji Z, Ammar S, Smiri LS, Vaulay MJ, Herbst F, Gallas B, Fievet F (2008) J Appl Phys 103:07E744
7. Acher O, Ledieu M, Abe M, Tada M, Matsushita N, Yoshimura M, Kondo K (2007) J Mag Mag Mater 310:2532

8. Kulkarni DC, Patil SP, Puri V (2008) Microelectron J 39:248
9. Kulkarni DC, Lonkar UB, Puri V (2008) J Mag Mag Mater 320:1844
10. Kumar A, Singh A, Yadav MS, Arora M, Pant RP, Thin Solid Films (In Press, Corrected Proof)
11. Wang JH, Liu YC, Liu DC, Yu YW, Guo FB (2009) J Mag Mag Mater 321:3646
12. Aphesteguy JC, Damiani A, DiGiovanni D, Jacobo SE (2009) Physica B 404:2713
13. Deka S, Joy PA (2006) Mater Chem Phys 100:98
14. Li X, Wang G (2009) J Mag Mag Mater 321:1276
15. Wu KH, Shin YM, Yang CC, Wang GP, Horng DN (2006) Mater lett 60:2707
16. Zi Z, Lei H, Zhu X, Wang B, Zhang S, Zhu X, Song W, Sun Y (2010) Mater Sci Eng B 167:70
17. Zahi S, Hashim M, Daud AR (2007) J Mag Mag Mater 308:177
18. He X, Song G, Zhu J (2005) Mater lett 59:1941
19. Priyadharsini P, Pradeep A, Rao PS, Chandrasekaran G (2009) Mater Chem Phys 116:207
20. Klug HP, Alexander LE (1997) X-ray diffraction procedures for poly-crystalline and amorphous materials. Wiley, New York
21. Sharma S, Verma K, Chaubey U, Singh V, Mehta BR (2010) Mater Sci Eng B 167:187
22. Smit J, Wijn HPJ (1961) Les Ferrites. Dunod, Paris
23. Herzer G (1995) Scr Metall Mater 33:1741